Int. J. Electrochem. Sci., 15 **(2020)** 9354 – 9377, doi: 10.20964/2020.09.95

International Journal of
ELECTROCHEMICAL
SCIENCE
www.electrochemsci.org

Exploring the corrosion inhibition effect of two hydrazone derivatives for mild steel corrosion in 1.0 M HCl solution via electrochemical and surface characterization studies

Abdelkarim Chaouiki[1], Maryam Chafiq[1], Mustafa R. Al-Hadeethi[2], Hassane Lgaz[3], RachidSalghi[1], Siham K. AbdelRaheem[4], Ismat H. Ali [4], Sara A. M. Ebraheem[4], Ill-Min Chung [3*], Shaaban K. Mohamed [5,6]*

[1] Laboratory of Applied Chemistry and Environment, ENSA, University Ibn Zohr, PO Box 1136, Agadir, Morocco;
[2] College of Education, Department of Chemistry, Kirkuk University, Kirkuk, Iraq;
[3] Department of Crop Science, College of Sanghur Life Science, Konkuk University, Seoul 05029, South Korea
[4] Department of Chemistry, College of Science, King Khalid University, P. O. Box 9004, Postal Code 61413, Abha, Kingdom of Saudi Arabia;
[5] Chemistry and Environmental Division, Manchester Metropolitan University, Manchester, United Kingdom;
[6] Chemistry Department, Faculty of Science, Minia University, El-Minia, Egypt;
[*]E-mail: hlgaz@konkuk.ac.kr (H. L.), imcim@konkuk.ac.kr (I-M. C.)

Received: 9 May 2020 / *Accepted:* 16 July 2020 / *Published:* 10 August 2020

In the last few decades, scientists have been interested in the deterioration and the corrosion of metals and their alloys in the acidic environment, which is widely used in various industrial applications. To develop new strategies that lead to control and inhibit the corrosion of metals, eco-friendly corrosion inhibitors have received a lot of interest in recent years. In this context, the main goal of the current study is to determine the functionality of two new synthesized hydrazone derivatives as potential corrosion inhibitors for mild steel in acidic HCl solution. To achieve this goal, the corrosion inhibition behavior of (E)-N'-(4-methoxybenzylidene)-2-(6-methoxynaphthalen 2-yl)propanehydrazide (HYD-3) and N'-cyclohexylidene-2-(6-methoxynaphthalen-2-yl)propanehydrazide (HYD-4) on MS was studied by employing electrochemical techniques in combination with surface characterization with the help of SEM-EDS analysis. As a result of these investigations, the two inhibitors exhibited excellent protection efficiency, and the best inhibition effect was shown by HYD-3 (90% at 5×10^{-3} M). Potentiodynamic polarization (PDP) results demonstrated that the two inhibitors are mixed-type inhibitors and that the adsorption isotherm of these molecules responds to the Langmuir model. Further analysis obtained by impedance spectroscopy (EIS) tests showed that the studied inhibitors make a positive impact on the mild steel corrosion process by increasing the polarization resistance with an increase in the concentration of the inhibitor. Another important practical result is that the SEM-EDS morphological information suggested that the studied compounds form protective films onto the MS surface. Further, the impact of solution temperature and immersion time on HYD-3 performance has

been evaluated. Finally, this work demonstrated significantly improved steel corrosion resistance and could pave a way to develop new-tagged inhibitors in this field.

Keywords: Corrosion inhibition; Mild steel; HCl; Hydrazone derivative; EIS; SEM/EDX.

1. INTRODUCTION

As the most basic metallic material in many industrial applications, mild steel (MS) has been widely used owing to its remarkable mechanical properties, extremely good resistance to tensile, its manufacturability, and economical price [1–3]. Much of the essential processes that MS has attracted considerable attention are the chemical and petrochemical industrial field. At the same time, different mineral acids like HCl, H_2SO_4, etc. are most commonly employed throughout these industries processes [4,5]. The main applicability of these acids is acid cleaning, descaling, and drilling operations in oil and gas exploration [6–8]. Nevertheless, during all the ineluctable activities based on the use of mild steel for construction and or fabrication in several vital sectors, the mild steel provides limited properties and applications in many aggressive environments especially those containing Cl^- ions due to corrosion attack. This major deterioration of MS behavior is more announced in the strongly acidic solution like chloride acid, which is very often used in many industrial applications [9–11]. Nowadays, the corrosion of mild steel brings huge economic losses and operational problems in most installations and industrial equipment [12,13]. As mentioned above, one could say that mild steel is the raw material for a significant proportion of industrial activity, and the reduction of free energy value is a fundamental reason for steel corrosion problems for any industrial system. Hence, all previous details make the mild steel a sensible material to the corrosion phenomenon and factors thought to be influencing MS corrosion have been explored in several studies. Up to now, a more substantial approach to decrease damage due to corrosion with the longer-term significance in the field of corrosion inhibition is the use of corrosion inhibitors due to its high efficiency, improved durability, and its low cost [14–16].

Until recently, a great deal of previous research into mild steel corrosion inhibition has focused on exploiting many eco-friendly corrosion inhibitors as an environmentally alternative to hazardous and toxic compounds to limit material deteriorations [17–20]. During mild steel corrosion process, these organic compounds play a crucial role, because it combines chemical action and electrostatic interaction between the inhibitor molecules and metal surface. These organic compounds also may play a fundamental role in the life cycle of mild steel and therefore addressing the issue of the economic effect of corrosion [21]. When it comes to the use of inhibitors, many inhibitors compounds have the inhibition effect for metal dissolution and meet the requirement to be environmentally friendly and biodegradable. This indicates a need to understand the various perceptions of inhibitor molecules that promoting environment safety and improving the inhibition efficiency. In this regard, extensive research has shown that environmentally friendly organic compounds containing phenyl rings, π bonds, and polar functional groups and heteroatoms (N, S, O, P), etc. considered to be the most effective corrosion inhibitors [22–24]. From this point of view, it is necessary to develop green

inhibitors with interesting characteristics that can answer different needs of industrial and environmental applications. For these reasons, new organic hydrazone derivatives based on Naproxen have been synthesized and evaluated for inhibiting corrosion of MS in the 1.0 M HCl solution. Naproxen is one of the most regularly used propionic acid derivatives for the treatment of pain, joint swelling and symptoms of arthritis. It is believed to work by blocking the action of cyclooxygenase (COX) involved in the production of prostaglandins that are produced in response to injury or certain diseases and cause pain, swelling and inflammation. However, its use is associated with some gastrointestinal side effects possibly caused by the free acidic group present [25]. One of the easier and safer ways to functionalize the carboxylate group in is its functionalization into hydrazones [26]. Hydrazones are a class of organic compounds characterized by the azomethine bond $R_1R_2C=NHNH_2$, where R_1, R_2 can be different functional group, so that hydrazones represent a very important starting materials in organic synthesis in addition to their biological importance.

In this perspective, this paper aims to evaluate the anti-corrosion effect of two new corrosion inhibitors, namely (E)-N'-(4-methoxybenzylidene)-2-(6-methoxynaphthalen 2-yl)propanehydrazide (HYD-3) and N'-cyclohexylidene-2-(6-methoxynaphthalen-2-yl)propanehydrazide (HYD-4) for mild steel corrosion in 1.0 M HCl solution. Their corrosion inhibition performance were evaluated by electrochemical impedance spectroscopy (EIS), potentiodynamic polarization (PDP) as well as weight loss (WL) studies. Besides, immersion time for 24 hours and temperature effects from 303K to 333K were studied through EIS and WL tests, respectively, and the stability of studied inhibitors is compared and discussed. The results obtained using all mentioned experiments were confirmed by morphological observations of MS substrate by SEM coupled with EDX analysis.

2. EXPERIMENTAL PROCEDURES

2.1. Mild steel preparation, electrolytes and inhibitors

This section describes the experimental approach and instrumentation utilized in this study. The material tested is mild steel known by its nuance, having good mechanical characteristics, and distinguished by its composition (wt %) given in Table 1.

Table 1. Elemental composition of the used mild steel coupons.

Atom	Content (%)
Fe	99.21
C	0.21
Si	0.38
Mn	0.05
S	0.05
P	0.09
Al	0.01

To prepare the electrolyte, a solution obtained from a 37% HCl acid of Sigma-Aldrich by diluting it with distilled water. So, the acidic environment used in this study is 1 M HCl solution. For the first step of these experiments, the polishing tool is a rotating disc containing 400, 800, 1200 and 1600 grit emery papers, which allow MS samples to mechanically polished. After the polishing of MS samples, they were cleaned with distilled water, followed by an acetone wash, and finally transferred immediately to the experimental tests. In this paper, the analyses were based on the prepared test solutions with a concentration range fixed between 10^{-4} and 5×10^{-3} M to examine the impact of HYD-3 and HYD-4 molecules on mild steel (MS) corrosion in terms of inhibitors performances. Full descriptions of the molecular structures, corresponding names and their characterization are given in Table 2. The full synthesis procedure is described in details in our recent paper [27].

Table 2. Molecular structures of HYD-3 and HYD-4 along with their characterization.

Inhibitors	Names and abbreviation
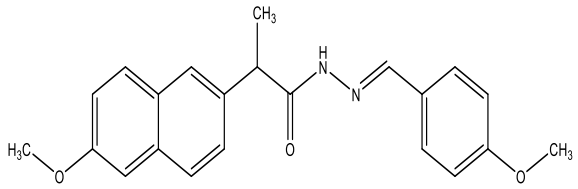	(E)-N'-(4-methoxybenzylidene)-2-(6-methoxynaphthalen-2-yl)propanehydrazide **(HYD-3)** m.p = 170-173^{0}C. IR (KBr): (C=O amide 1653 cm^{-1}), (N-H 3195 cm^{-1}), (-C=N 1602 cm^{-1}). ^{1}H NMR (400MHz, DMSO): δ = 1.4 (d, 3H, CH_3), 3.3 (q, 1H, C-H), 3.8 (s, 6H, OCH_3), 8.3 (s, 1H, -CH=N-), 10.4 (s, 1H,-NH), 7.1-8.0 (m, 9H, aromatic protons). ^{13}C-NMR δ =18 (CH_3), 43 (C-H aliphatic), 56 (2OCH_3), 106-156 (14 aromatic carbons), 161(C=N), 173 (C=O amide).
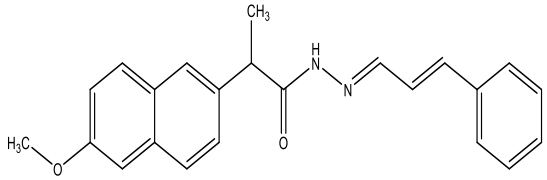	2-(6-methoxynaphthalen-2-yl)-N'-((1E,2E)-3-phenylallylidene)propanehydrazide **(HYD-4)** m.p =190-192 ^{0}C. IR (KBr): (C=O amide 1666 cm^{-1}), (N-H 3236 cm^{-1}), (-C=N 1606 cm^{-1}), (C-H aliphatic 2867-2952 cm^{-1}).^{1}H NMR (400 MHz, DMSO): δ = 1.4 (d, 3H, CH_3), 3.4 (q, 1H, C-H), 3.8 (s, 3H, OCH_3), 10.0 (s, 1H, -NH), 7.1-7.8 (m, 6H, aromatic protons), 7.8 (s, 1H, -CH=N). ^{13}C-NMR δ =18 (CH_3), 44 (C-H aliphatic), 55 (OCH_3), 106-155 (10 aromatic carbons), 158 (C=N), 171 (C=O amide).

2.3. Weight loss (WL) study

Weight loss is an important method designed to evaluate and determine the corrosion rate of MS. Hence, the inhibition effect of studied inhibitors was primarily studied by weight loss method owing to its simplicity and high consistency**.** WL measurements were performed in a stagnant aerated solution. We choose rectangular substrates of MS with dimensions of 2.5 x 2 x 0.9 cm^3. As explained earlier, before each experiment, samples were prepared and thoroughly cleaned. During all weight loss tests, the MS samples were weighed with a precision balance and then immersed in HCl solution with and without different inhibitor concentrations for an immersion period of 24 hours at the temperature range from 303 ± 2 K to 333 K ± 2 K. It would be interesting to repeat the experiments described here

to confirm the results and only the average values were considered. After attaining 24h of immersion time, the MS coupons were retrieved from test solutions, rinsed with distilled water, and weighted again. All experimental methodology based on weight loss measures and MS specimens preparation were carried out under the ASTM standard conditions [28]. Weight difference before and after immersion in test solutions is estimated and represented by W (in gram) to calculate the corrosion rate (C_{RW} in mg cm^{-2} h^{-1}) by using the following equation (1):

$$C_{RW} = \frac{K \times W}{A \times t \times \rho} \quad (1)$$

For K, A, and ρ parameters under the standard condition of ASTM; K was used as constant and equal to 8.76×10^4, A is exposed MS area (A) in cm^2 and ρ represents the density and equal to 7.86 g cm^{-3}, while t denotes immersion time in hours.

The corrosion inhibition efficiency of the tested compounds and their surface coverage (θ) was determined using the average mass loss estimated, as given below by using equations 2 and 3 [29–31]:

$$E_{WL}(\%) = \left[\frac{C^{\circ}_{RW} - C^{HYD}_{RW}}{C^{\circ}_{R}}\right] \times 100 \quad (2)$$

$$\theta = \frac{E_{WL}(\%)}{100} \quad (3)$$

Where C°_{RW} and C^{HYD}_{RW} corresponds to corrosion rates of the mild steel in the blank solution and after the addition of different concentrations of HYD-3 and HYD-4 inhibitors, respectively.

2.4. Electrochemical studies for corrosion inhibition

All electrochemical tests have been conducted in a corrosion cell with three different functional electrodes. The MS is used as working electrode, which has a surface area of 1 cm^2, an electrode type that is saturated calomel was used as the reference electrode, and the auxiliary electrode (counter-electrode) is a platinum (Pt). It can be noted that the electrochemical system discussed above was performed using Wuhan Corrtest Instruments Corp., Ltd. (Hubei, China) controlled with a computer, and the electrochemical results were acquired using electrochemical analyzer software. Mild steel electrode has been soaked in the corrosive solution, and the electrochemical experiments were run after 30 min at 303 K ± 2 K, to acquire a relatively stable value obtained by the open circuit potential (OCP). Also, the analysis obtained for each method, including EIS and polarization curves are estimated for 24 hours of immersion time in a tested solution. In this way, the EIS tests were done at premeasured OCP by superimposing a sinusoidal AC potential perturbation of 5 mV in the frequency range of 10 mHz to 100 kHz. For the electrochemical characterization of mild steel by PDP curves test, the electrode potential was recorded automatically from -700 to -300 mV versus SCE with a scan rate of 0.5 mV/s. Some possible methods and programs using to analyze experimental results, but EC lab software is widely applied to extract the analyses and simulations of the test results obtained by EIS

study. Once the PDP curves were extracted, the electrochemical parameters were estimated from Tafel plots with the aid of Tafel extrapolation method.

2.5. Surface morphology study (SEM/EDS)

The scanning electron microscope, coupled with the EDX analysis, was introduced to observe and analyze the surface of mild steel after an immersion time of 24 hours in 1.0 M HCl and the with and without inhibitors. Besides, the EDX spectrum was analyzed to explore and provide information on the elemental constituents of layers formed on MS before and after the addition of inhibitors molecules.

3. RESULTS AND DISCUSSION

3.1. Comparison of inhibition effects using weight loss measurements

3.1.1. Effect of HYDs concentrations

The inhibition effects of HYD-3 and HYD-4 on mild steel substrates were firstly investigated by weight loss studies to evaluate the anti-corrosive proprieties of these inhibitors in the acid solution. Using this method, the effect of studied compounds concentration on the corrosion rate of MS was investigated at a fixed temperature. Table 3 compares the results obtained from the preliminary analysis of concentrations effect of HYD-3 and HYD-4 on both corrosion rate and inhibition efficiency for 24 h of immersion at 303 K ± 2 K. Closer inspection of Table 3 shows that after addition of inhibitors to HCl medium, the corrosion rate (C_{RW}) of MS decreases. In contrast, an increase in inhibition efficiencies was observed. Also, data in Table 3 indicates that the two inhibitors were proven to be highly efficient corrosion inhibitors for MS, reaching a maximum value of 91% and 89% in the presence of HYD-3 and HYD-4, respectively, at $5x10^{-3}$ M. From these results, it is important to note that there is clear evidence that the two inhibitors have more ability to be adsorbed on the MS surface by increasing inhibitor concentration meaning that the surface area coverage of MS is significantly increased. Therefore the MS dissolution is considerably decreased. Based on this, the attempt was made to quantify the association between the excellent protection against steel corrosion by the studied compounds and the special molecular proprieties of these compounds. In this context, it is supposed that the presence of π-bonds in aromatic moieties, acyl group, imine group (C=N) on both inhibiting molecules, as well as methoxy groups and molecular size of molecules are most likely attributed to aid us to interpret and compare the performance of these inhibitors. Perhaps the most important distinguishing between the inhibitory efficacies of the two studied compounds could be explained by the functionality of the methoxy group (important electron-donating group) which enhances the adsorption phenomenon onto the MS surface [32]. Most importantly, it is suggested that during the corrosion inhibition process by organic inhibitors, the electron-donating groups promote the complexation with mild steel surface leading to a complete blockage of corrosion of active sites by forming a protective layer on the mild steel surface [33].

Table 3. Corrosion parameters for mild steel in 1.0 HCl at different concentrations of HYD-3 and HYD-4 for 24 hrs. at 303 K estimated from weight loss (±SD).

Inhibitor	Concentration (mol/L)	W (mg/cm^2 × h)	Θ	η_{WL} (%)
HCl	1	1.135 ± 0.0121	-	-
HYD-3	5×10^{-3}	0.102 ± 0.0015	0.91	91
	1×10^{-3}	0.170 ± 0.0025	0.85	85
	5×10^{-4}	0.204 ± 0.0030	0.82	82
	1×10^{-4}	0.238 ± 0.0035	0.79	79
HYD-4	5×10^{-3}	0.136 ± 0.0085	0.88	88
	1×10^{-3}	0.204 ± 0.0025	0.82	82
	5×10^{-4}	0.249 ± 0.0047	0.78	78
	1×10^{-4}	0.295 ± 0.0050	0.74	74

3.1.2. Temperature effect on inhibition performances HYDs

Questions have been raised about the stability of organic compounds under certain conditions during corrosion inhibition process. There has been a surge of interest in the effects of temperature as an important factor found to be influencing the inhibition efficiency for several organic compounds. Furthermore, the precise effect of temperatures on the inhibition process perhaps increasing or reducing the aggressiveness of electrolytes solutions and therefore influence both the efficacy of inhibitor and prolonged use of mild steel in many industrial applications. For these reasons, it is important to examine and to get more information into the impact of temperature on the inhibition mechanism in terms of inhibitor's stability as indicated above. In this section, WL study has been performed to determine the possible effects of temperature ranging from 303 to 333 K for both the corrosion rate of MS and the protection efficiency of the studied inhibitor. Using this approach, Table 4 illustrates the effect of temperature on MS dissolution in the absence and presence of different concentrations of (HYD-3) hydrazones. As Table 4 shows, on the one hand, the corrosion rate values of mild steel surface for both inhibited and uninhibited system are increased with the increase of temperature, and on the other hand, a decrease in protection efficiency of HYD-3 with the rise in temperature was observed. This is mainly due to acid-catalyzed molecular fragmentation or hydrolysis of the studied inhibitor at high temperatures, and therefore, the adsorption mechanism of inhibitor is influenced [34–36]. More interesting, from this data (Table 4), there is no significant difference between inhibition efficiency obtained at the same concentrations despite the rise in temperature. For example, the protection efficiency of HYD-3 decreases from 91% to 88% at $5x10^{-3}$ M from 303 K to 333 K, respectively. Also, below this concentration, no significant decreases were observed in terms of inhibition efficiencies. Comparison of the findings with those of other studies [37,38] confirms that the maximum performance of HYD-3 hydrazone is important and could effectively inhibit mild steel dissolution under aggressive environment (HCl) even at high temperatures.

Furthermore, the key aspects of the temperature effect can be best evaluated and examined using the Arrhenius plots. Utilizing this type of analysis approach to determine the activation and thermodynamic parameters are essential and also useful to address the long term temperature effects during the corrosion inhibition process. The obtained curves from Arrhenius equation and the transition state functions described below (equations 4&5) [37,38] were fitted to estimate and shed more light on the thermodynamic parameters such as enthalpy ΔH^* of activation, apparent entropy ΔS^* and activation energy E_a for the MS corrosion in 1.0 M HCl in the absence and presence of different concentrations of HYD-3 hydrazone.

$$C_{WL} = K \times e^{\frac{-Ea}{RT}} \quad (4)$$

$$C_{WL} = \frac{RT}{Nh}\exp(\frac{\Delta S^*}{R})\exp(\frac{\Delta H^*}{RT}) \quad (5)$$

In the above equations, the adsorption equilibrium constant is abbreviated K_{ads}, T represents the working temperature expressed in (K), R signifies the universal gas constant, it is worth 8.3144620 J mol^{-1} K^{-1}, h is Planck's constant and N denotes the number of Avogadro.

Arrhenius plots illustrated in Figure 1 (a-b) explore the relationship between ln C_{WL} and ln C_{WL}/T vs. absolute temperature (1/T) for MS corrosive dissolution with and without hydrazones inhibitors. Table 5 displays multiple thermodynamic parameters calculated using the slope and intercept estimated from the Arrhenius plots for analyzing the corrosion inhibition mechanism to give a full picture of the protectiveness impact of HYD-3 in HCl solution at various temperatures. This Table is quite revealing of several observations. First, the calculated (E_a) values are generally seen as a factor strongly related to the concentrations of inhibitors, and all values of E_a for inhibited solution are greater when compared to those of uninhibited solution.

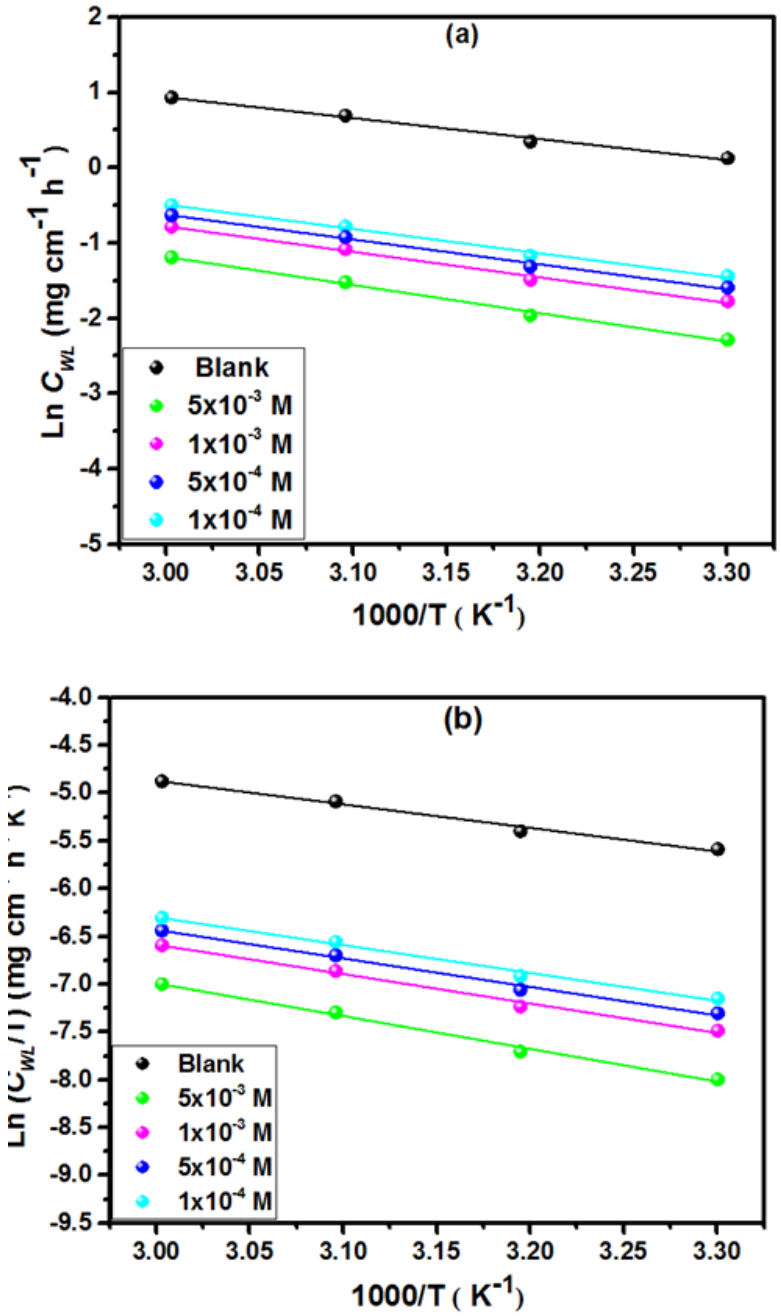

Figure 1. Arrhenius plots; ln C_{WL} *vs.* 1/T (a) and ln C_{WL}/T vs 1/T (b) for MS electrode with and without various concentrations of HYD-3 in 1.0 M HCl at 303 K.

Table 4. The effect of temperature toward the corrosion rate (±SD) and inhibition efficiency for MS steel in 1.0 M HCl in the absence and presence of HYD-3.

Solution		Temperature	Corrosion rate	Inhibition efficiency
		K	mg/cm^2 ×h	%
Blank	1.0 M HCl	303	1.135 ± 0.0121	-
		313	1.416 ± 0.0215	-

		323	1.998 ± 0.0214	-
		333	2.539 ± 0.0316	-
HYD-3	**5×10^{-3}**	303	0.102 ± 0.0015	91
		313	0.141 ± 0.0062	90
		323	0.219 ± 0.0079	89
		333	0.304 ± 0.0070	88
	1×10^{-3}	303	0.170 ± 0.0015	85
		313	0.226 ± 0.0059	84
		323	0.339 ± 0.0062	83
		333	0.457 ± 0.0056	82
	5×10^{-4}	303	0.204 ± 0.0030	82
		313	0.269 ± 0.0078	81
		323	0.399 ± 0.0062	80
		333	0.533 ± 0.0032	79
	1×10^{-4}	303	0.238 ± 0.0035	79
		313	0.311 ± 0.0056	78
		323	0.459 ± 0.0063	77
		333	0.609 ± 0.0040	76

This rise in E_a values in inhibited solution (with HYD-3) when correlated with those of the blank indicates that the dissolution process of MS in the inhibited system is slower because the system with inhibitors stimulates the energy barrier for corrosion reaction [39,40]. The second observation from the obtained data was that the ΔH^* values increase and ΔS^* values are superior to that of the uninhibited system, and it is negative. So, it can be suggested that the positive sign of ΔH^* shows the endothermic nature of MS dissolution and the negative values of ΔS^* could be attributed to the fact that there is a decrease in disorder during the switch from reagents to the activated complex during the corrosion process [41]. Finally, for reference to specific studies carried out in this field [30,42,43], all these findings suggesting the adsorption of studied inhibitor on mild steel surface which is a quasi-substitution phenomenon between HYD-3 in HCl solution and H_2O molecules present on the mild steel interface.

Table 5. The values of corrosion kinetic parameters for mild steel in the presence and absence of various concentrations of HYD-3.

	Blank	**HYD-3**			
		5×10^{-3}	**1×10^{-3}**	**5×10^{-4}**	**1×10^{-4}**
E_a (kJ mol^{-1})	23.12	31.15	28.26	27.45	26.88
ΔH_a	20.48	28.51	25.62	24.81	24.24

(kJ mol^{-1})					
ΔS_a (J mol^{-1} K^{-1})	-176.48	-170.02	-175.33	-176.48	-177.07
E_a - ΔH_a (kJ mol^{-1})	2.64	2.64	2.64	2.64	2.64

3.2. Potentiodynamic polarization plots measurements

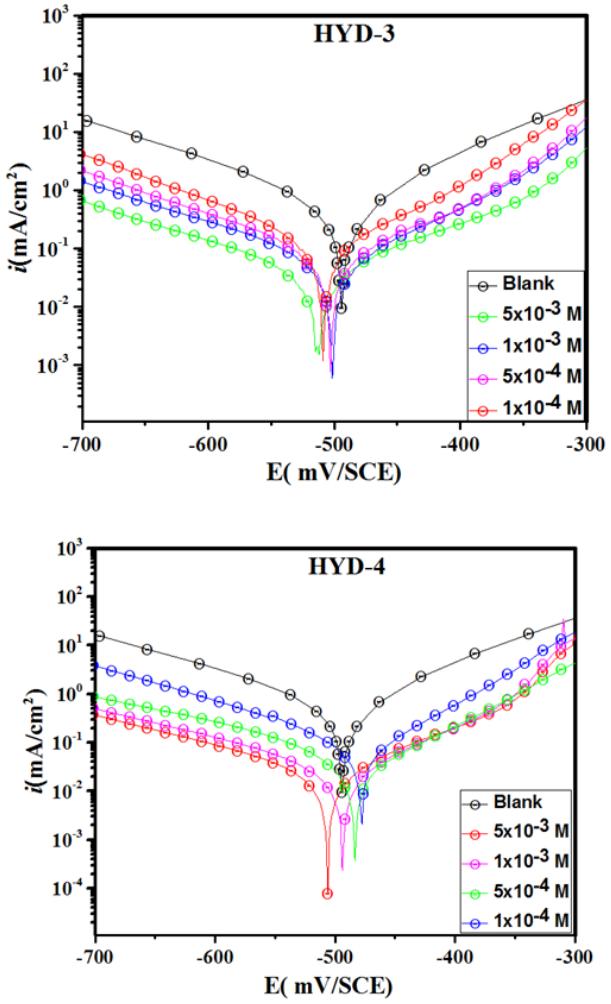

Figure 2. Recorded plots of PDP for MS in HCl solution with and without HYD-3 and HYD-4 at 303K.

Exploring the relationships between corrosion current density and corrosion potential is important for our heightened understanding of the reactions occurring on the surface of mild steel. To this end, we conducted a PDP study in detail. This study provides important information on the kinetics of the anodic and cathodic reactions of the corrosion process. After a 30 min immersion time in the acid solution, PDP plots of MS coupons immersed in uninhibited and inhibited solutions were made. Table 6 compiles the data calculated from the Tafel plots (Figure 2), including corrosion potential (E_{corr}) and corrosion current density (i_{corr}) as well as the cathodic and anodic slopes of Tafel

(βc, βa). From the calculated values of corrosion current density, the inhibition efficiency was estimated by using the following equation:

$$E_{PDP}(\%) = \left[1 - \frac{i_{corr}^{HYD}}{i_{corr}^{\circ}}\right] \times 100 \quad (7)$$

Where i_{corr}° and i_{corr}^{HYD} represent the corrosion current densities respectively without and with the addition of different concentrations of HYD hydrazones.

Table 6 shows that the presence of two compounds has significantly shifted the corrosion current densities to lower values, with the result that the corrosion of steel is strongly inhibited with the addition of these inhibitors. Besides, it has been noticed that with increasing inhibitor concentrations, the corresponding protective efficacy of HYD-3 and HYD-4 increases significantly. Also, there is no significant change in the potential corrosion values in Figure 3 since the displacement in E_{corr} between the blank solution and the solution containing the inhibitors is not large. Based on this result, the effect of corrosion inhibition by the studied compounds is generally mixed, i.e. it affects both the development of cathodic hydrogen and the dissolution of the active metal on the anode branch [44,45]. It is possible that the unremarkable variation in the anodic and cathodic slopes of Tafel seen in Table 6 in the presence of HYD inhibitors could be attributed to the fact that the major anodic and cathodic reactions during the dissolution mechanism of mild steel are controlled without modification [46]. However, the difference in per cent inhibition efficacy for the two inhibitors at the same concentrations can be seen in Table 6. This is due to the synergistic effect of the different molecular properties of these inhibitors, which adsorb to the surface of the steel [30,47–49]. This is well verified by the results of previous studies which demonstrate a strong and consistent association between the unique characteristics of these molecules and their high protective performance, which proves that hydrazone derivatives with more interesting properties in their molecular structures have a strong interaction with the MS surface.

Table 6. Potentiodynamic parameters values estimated from PDP curves of MS in 1.0 M HCl solution in the presence and absence of various inhibitors concentrations at 303 K.

Inhibitor	Concentration (M)	$-E_{corr}$ (mV vs. SCE)	$-\beta_c$ (mV dec^{-1})	$-\beta_c$ (mV dec^{-1})	i_{corr} (µA cm^{-2})	η_{PDP} (%)
Blank	1.0	496 ± 0.4	150 ± 3.5	92 ± 5.7	564 ± 2.3	-
HYD-3	5×10^{-3}	515 ± 0.2	130 ± 6.8	84 ± 7.4	54 ± 5.8	90
	1×10^{-3}	503 ± 0.7	144 ± 3.4	88 ± 5.1	81 ± 6.2	86
	5×10^{-4}	505 ± 0.3	136 ± 4.2	82 ± 2.8	92 ± 4.2	83
	1×10^{-4}	511 ± 0.6	139 ± 5.8	79 ± 3.9	108 ± 3.5	80
HYD-4	5×10^{-3}	508 ± 1.1	168 ± 5.9	78 ± 6.8	89 ± 5.2	88
	1×10^{-3}	496 ± 0.4	160 ± 2.8	70 ± 7.1	114 ± 5.7	84
	5×10^{-4}	483 ± 1.4	154 ± 8.1	76 ± 4.9	132 ± 4.3	79
	1×10^{-4}	473 ± 0.8	170 ± 8.1	74 ± 5.7	67 ± 6.5	76

3.3. Electrochemical impedance spectroscopy (EIS) measurements

3.3.1. Concentration effect

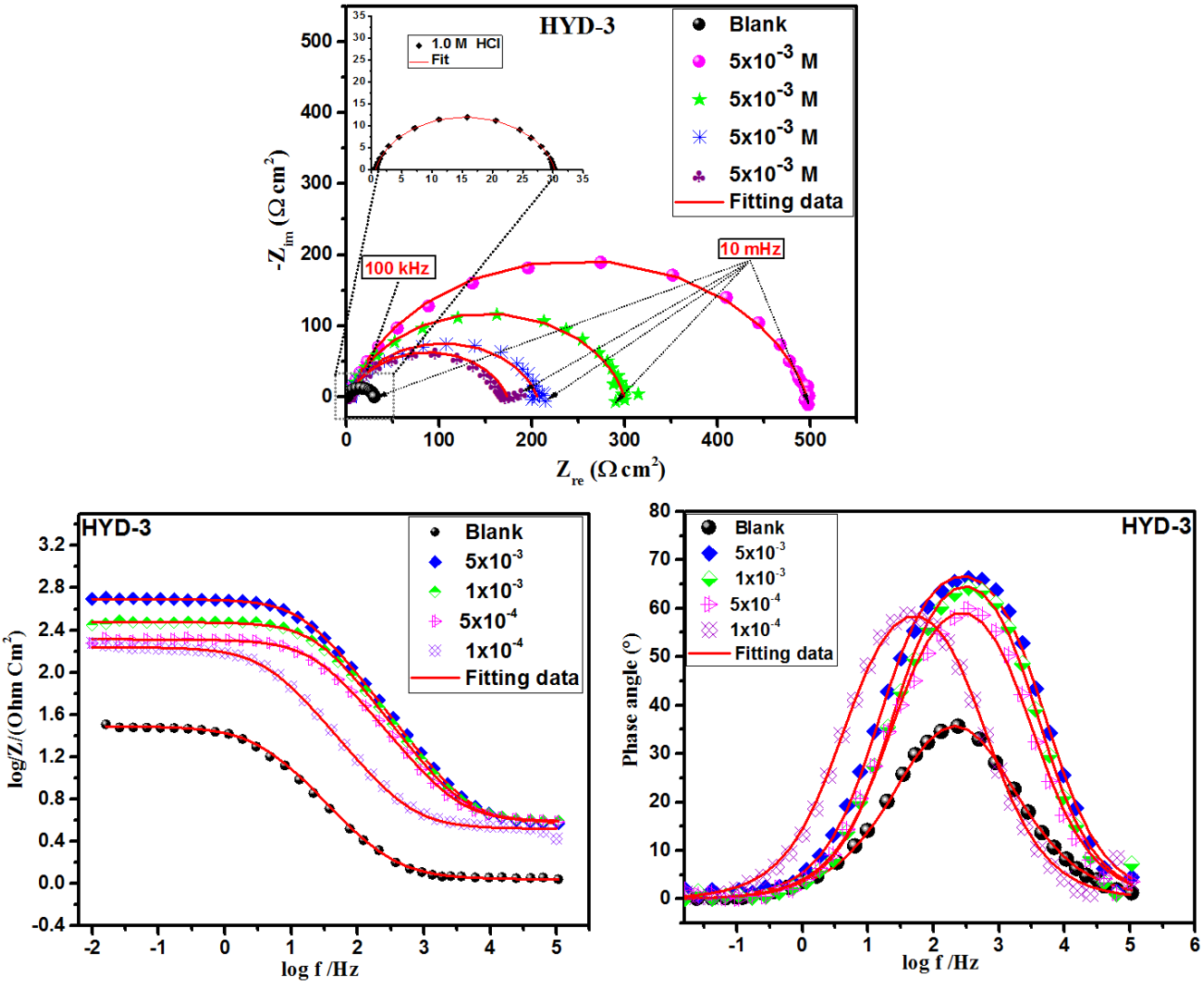

Figure 3. EIS curves and Bode diagrams of mild steel substrate immersed in 1.0 M HCl solution without and with various concentrations of HYD-3 inhibitor.

Impedance measurements have been performed for MS in 1.0 M HCl with and without several concentrations of HYD-3 and HYD-4 inhibitors. Nyquist plots of uninhibited and inhibited solutions containing variable concentrations of the inhibitory molecule are illustrated in Figures 4 and 5. Based on the following equation, the double-layer electrical capacity (C_{dl}) for each case was calculated [6,50]:

$$C_{dl} = \sqrt[n]{Q \times R_p^{1-n}} \quad (8)$$

With *n* indicating the phase shift that allows calculating the surface heterogeneity of mild steel [51,52]. Based on the EIS technique, for the determination of inhibitory efficacy, the following formula is used:

$$E_{EIS}(\%) = \left[\frac{R_p^{HYD} - R_p^{\circ}}{R_p^{HYD}} \right] \times 100 \qquad (9)$$

Where R_p° and R_p^{HYD} signify the polarization resistance in the blank and with the addition of inhibitors, respectively.

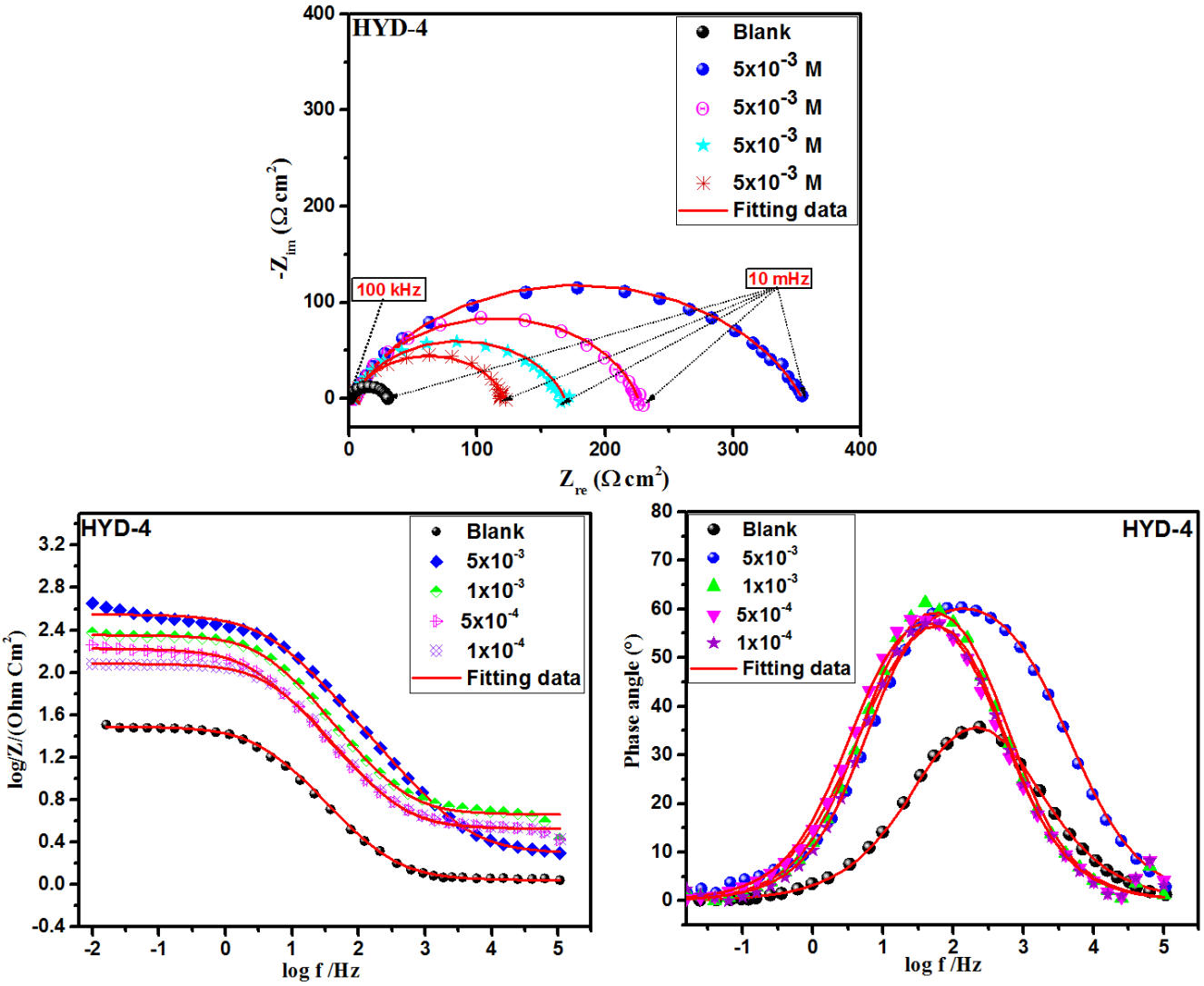

Figure 4. EIS curves and Bode diagrams of mild steel substrate immersed in 1.0 M HCl solution without and with various concentrations of HYD-4 inhibitor.

The double-layer capacitance (C_{dl}) derived from the CPE, the efficacy, and other parameters are also presented in Table 7. EIS spectra with the equivalent circuit exposed in Figure 5 were adjusted to obtain R_p values significant for corrosion resistance. In previous works, it has been proven why the polarization resistor is used as an alternative to the charge transfer resistor [2,53]. Mild steel EIS

diagrams, taken without inhibitor and in the inhibited solutions after 30 min of immersion time, show the existence of what appeared to be a single capacitive loop with increasing size as the inhibitor concentration increases due to the charge transfer process. This produces a thin film on the metal surface, which is strengthened in the presence of inhibitors. As inhibitor concentration increases, R_p values increase while C_{dl}values decrease, according to Table 7. High polarization resistance is linked to a slower corrosion system [54]. This is well in line with the behavior of the phase shift (n). Based on these results, it is suggested that adsorption takes place on the mild steel surface leading to the formation of a protective thin film that inhibits the dissolution of MS in HCl medium. The phase angle values for the two inhibitors used were always greater than white but less than -90°, indicating the non-ideal capacitor.

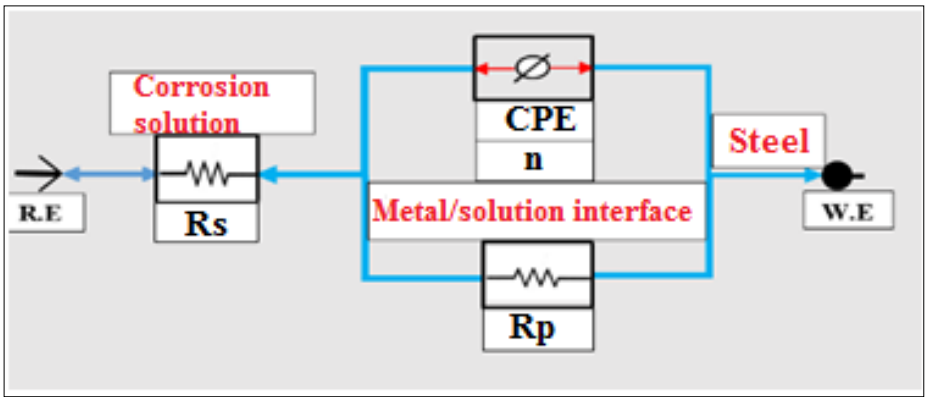

Figure 5. Equivalent circuit model applied to fit and simulate the EIS experiments.

Table 7. Electrochemical parameter values obtained after fitting the impedance spectra of MS in 1.0 M HCl with and without various concentrations of HYD-3 and HYD-4 at 303 K.

Inhibitor	Concentration (M)	R_p (Ωcm^2)	n	$Q \times 10^{-4}$ ($S^n \Omega^{-1} cm^{-2}$)	C_{dl} ($\mu F cm^{-2}$)	Goodness of fit (χ^2) $\times 10^{-3}$	η_{EIS} (%)
Blank	1.0	29 ± 1.5	0.89 ± 0.005	1.761 ± 0.0025	92	0.33	-
HYD-3	5×10^{-3}	488 ± 1.9	0.83 ± 0.003	0.2523 ± 0.0014	10	4.36	93
	1×10^{-3}	293 ± 1.6	0.84 ± 0.005	0.3731 ± 0.0018	15	4.48	89
	5×10^{-4}	200 ± 1.2	0.82 ± 0.008	0.5696 ± 0.0032	21	3.79	85
	1×10^{-4}	163 ± 1.5	0.81 ± 0.006	0.8094 ± 0.0086	29	3.21	81
HYD-4	5×10^{-3}	352 ± 1.7	0.81 ± 0.001	0.3675 ± 0.0048	13	1.38	91
	1×10^{-3}	212 ± 1.9	0.80 ± 0.002	0.5461 ± 0.0039	17	4.18	86
	5×10^{-4}	165 ± 1.5	0.79 ± 0.007	0.7434 ± 0.0080	23	3.56	82
	1×10^{-4}	118 ± 1.9	0.82 ± 0.006	0.9281 ± 0.0096	34	6.88	75

3.3.2. Immersion time effect on the performance of HYD-3

To further confirm the successful performance of hydrazone derivatives to inhibit the corrosion of mild steel, additional studies will be needed to develop a full picture into inhibition performances of these compounds under various conditions having a considerable impact on the inhibitory efficacy. Now, this part of this work focuses on the effect of immersion time, which is among the most important factors influencing the performance of inhibition. For this, the effect of immersion time on inhibition activity of HYD-3 compound has been performed using EIS study and then evaluated to describe some of the more recent developments related to the variation of the performance of hydrazone derivatives with the immersion time. More specifically, EIS measurements can determine the tendency of HYD-3 to be more stable when placed in a specific corrosive environment (HCl) after different immersion times; 30 min, 6h, 12h, and 24h at 303 K. Figure 6 shows the EIS plots obtained for the uninhibited case and with the presence of $5x10^{-3}$ M of HYD-3 as a function of immersion time.

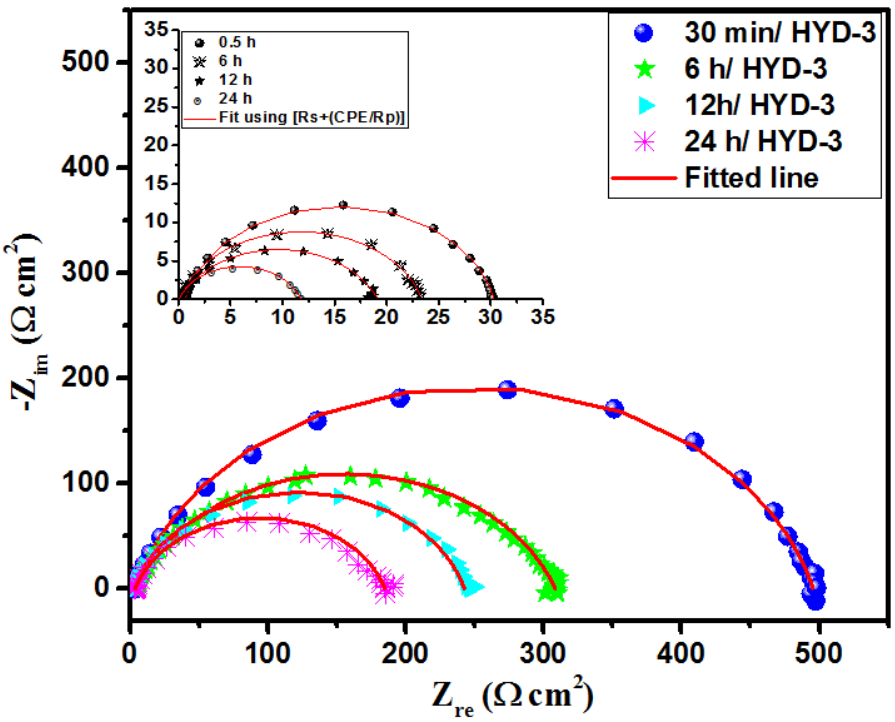

Figure 6. Nyquist curves of mild steel substrate immersed in 1.0 M HCl solution without and with 5x10-3 M of HYD-3 at various times.

Table 8 displays the results obtained from EIS curves related to electrochemical parameters of the studied systems. From the data in Figure 6, it is apparent that the corrosion behavior of MS with the variation of immersion time characterized by the appearance of a single capacitive loop for the two studied systems. Furthermore, from this data (Table 8), we can see that the polarization resistance of mild steel in the presence of HYD-3 decreases as the immersion time increases; from 12 Ω cm^2 for the blank solution to 265 Ω cm^2 with the presence of HYD-3 (at $5x10^{-3}$ M) after 24 h of immersion time.

Besides, the HYD-3 shows excellent inhibition performance over a long test time. Also, it can be noted that the protection efficiency stays 93% even when increasing the immersion time to 24 h.

What is important for us to recognize here, is the more stability of inhibition efficiency with time in the presence of HYD-3 inhibitor, which indicates that HYD-3 has much stronger adsorption ability with mild steel surface through free electrons of the heteroatom present in that inhibitor. Therefore, the protective film formed over the surface of MS becomes very compact and uniform, which exhibits superior stability to improve the efficiency at longer immersion time.

Table 8. EIS parameters for mild steel in 1.0 M HCl without and with HYD-3 vs. immersion time.

Inhibitor	Time (H)	R_p (Ωcm^2)	n	$Q \times 10^{-4}$ ($S^n \Omega^{-1} cm^{-2}$)	C_{dl} ($\mu F cm^2$)	Goodness of fit (χ^2) $\times 10^{-3}$	η_{EIS} (%)
Blank	0.5	29 ± 1.5	0.89 ± 0.005	1.7610 ± 0.0025	92	0.33	-
	6	23 ± 2.5	0.84 ± 0.007	2.5114 ± 0.0037	94	2.45	-
	12	18 ± 1.7	0.83 ± 0.004	2.9866 ± 0.0084	102	3.24	-
	24	12 ± 2.9	0.88 ± 0.003	3.0891 ± 0.0031	144	1.14	-
HYD-3	0.5	488 ± 1.9	0.83 ± 0.003	0.2523 ± 0.0014	10	4.36	93
	6	322 ± 1.3	0.82 ± 0.002	0.4451 ± 0.0032	17	5.18	92
	12	238 ± 1.6	0.83 ± 0.003	0.5759 ± 0.0088	23	4.95	92
	24	181 ± 2.8	0.81 ± 0.007	0.7723 ± 0.0032	30	2.50	93

3.4. Determination of adsorption type

Table 9. Thermodynamic parameters of MS corrosion in 1.0 M HCl solution with the presence of HYD-4 and HYD-3 compounds.

Inhibitor	**Temperature (K)**	**K_{ads} (L/mol)**	**R^2**	**ΔG^0_{ads} (kJ/mol)**	**ΔH_a (kJ mol^{-1})**	**ΔS_a (J mol^{-1} K^{-1})**
HYD-4	303	20919	0.999	-35.16	-	-
HYD-3	303	18424	0.999	-38.09	-70.90	-10.83
	313	18001	0.999	-37.01		
	323	17584	0.999	-35.93		
	333	17172	0.999	-34.84		

Inhibitory organic molecules are chosen based on their potential ability to adsorb on the MS surface in an acidic environment. The adsorption type isotherms are typically applied to obtain information regarding the type of adsorption of organic inhibitor molecules on a mild steel surface during corrosive process conditions. Testing has been performed on several different adsorption isotherms such as Langmuir, Temkin and Frumkin. The Langmuir model proved to be the best description (Figure 7a). Its standard equation is given as follows:

$$\frac{C_{inh}}{\theta} = \frac{1}{K_{ads}} + C_{inh} \quad (10)$$

In which C_{inh} signifies the inhibitor concentration, K_{ads} means a constant of adsorption equilibrium while θ denotes the area coverage.

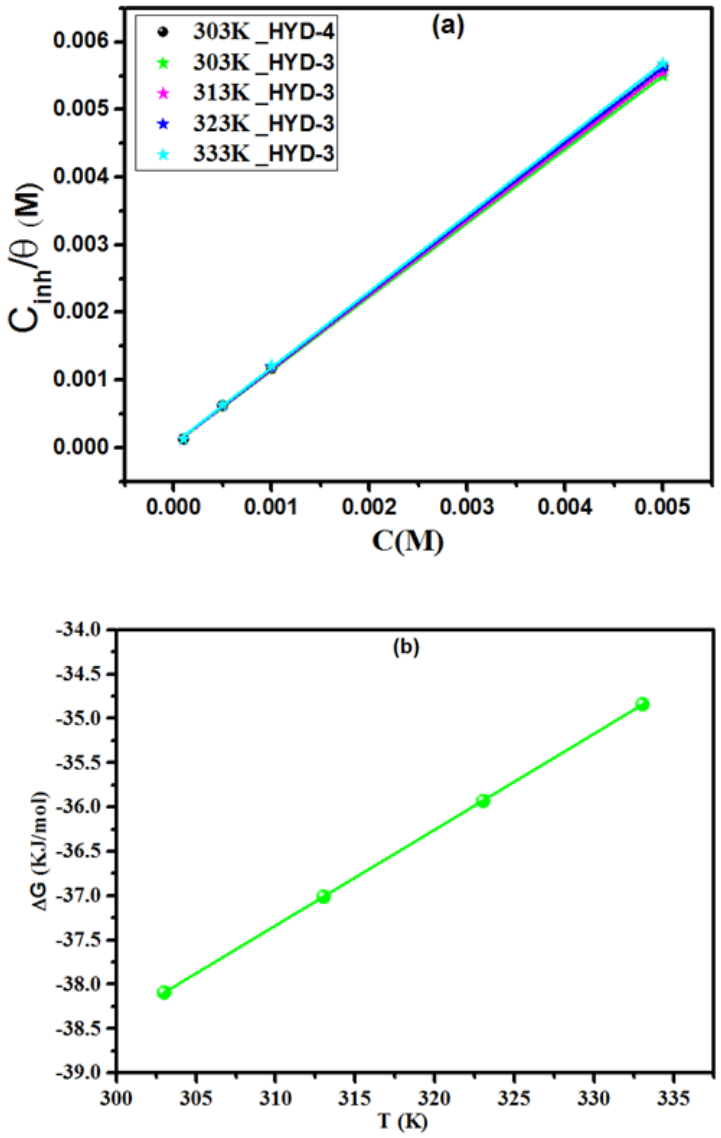

Figure 7. (a) Langmuir adsorption isotherm models and (b) the variation of standard Gibbs free energy of HYD-3 with temperature for the adsorption of inhibitor on MS in 1.0 M HCl.

The value of K_{ads}, which is obtained from the intercepts in Figure 1, is related to standard free adsorption energies (ΔG°_{ads}) as follow [55]:

$$K_{ads} = \frac{1}{55.5}\exp\left(\frac{-\Delta G_{ads}}{RT}\right) \quad (11)$$

In the above equation, 55.5 is the water molar concentration measured in mol L^{-1}, where T indicates the temperature of the aqueous solution, and R is known as the universal gas constant. The adsorption parameters ΔH°_{ads} and ΔS°_{ads} on the MS surface is computed according to the next relationship [56]:

$$\Delta G^{\circ}_{ads} = \Delta H^{\circ}_{ads} - T\Delta S^{\circ}_{ads} \quad (12)$$

Standard free Gibb adsorption energy is shown in Table 9 with significant negative values, and high values as an indication of the marked interaction of the two studied compounds with the MS surface and the spontaneity of the adsorption process. Here, the free energy of adsorption could provide useful information on the mode of adsorption involved in the interaction of hydrazone derivatives with the mild steel surface. The ΔG°_{ads} values listed in the Table show that the adsorption is of a mixed type. The values of $\Delta G^{\circ}_{ads}$of HYD-3 have been determined at various temperatures; the results are presented in Figure 7b. The negative values ΔH°_{ads} and ΔS°_{ads} pretend that the inhibitor's adsorption on metal is perceived as an exothermic reaction that is confirmed by a reduction in entropy.

3.5. SEM-EDX analysis

In this work, more research analysis is required, on the one hand, to provides more insight into the corrosion inhibitor effect on the metal surface, and on the other hand to support the electrochemical findings. For this purpose, scanning electron microscopy analysis was used to investigate the morphological surface of mild steel samples after being immersed in HCl solutions without and with the addition of inhibitor for 24 h of immersion at 303K. The surface morphologies of processed mild steel surfaces for the non-inhibited solution, and the one inhibited contains 5×10^{-3} M of HYD-3 inhibitor are displayed in Figure 8 (a-b). As Figure 9 shows, there is a significant difference between the two SEM images. From Figure 9a, it clear that the surface of mild steel is heavily impacted owing to accelerated corrosion attack in aggressive solutions, meaning that the surface of the specimen is significantly deteriorated and corroded. On the other hand, corrosion is reduced in the presence of HYD-3 at the optimum concentration as shown in Figure 9b, indicating that the mild steel surface is greatly protected, which could be due to the adsorption of molecules and the formation of a protective layer at the MS/ solution interface.

Furthermore, with the aid of EDX analysis, the elemental composition of the mild steel samples before and after the addition of HYD-3 was identified to provide comprehensive visual insights regarding this inhibitor's effect on the morphology of MS surface in term of the corrosion product present on the MS surface. The EDX spectrum with no inhibitor (Figure 8c) displays the peaks intensity of Fe, Cl, and O elements. However, compared with those of inhibited solution, the chlorine and oxygen peaks decrease, as shown in the EDX spectrum (Figure 8d). Moreover, another new peak appeared at this spectrum related to the nitrogen. The decrease of O and Cl peaks intensity and

appearance of N in the inhibited system confirms the presence of HYD-3 inhibitor on the MS surface, and it can be adsorbed onto the steel and then formed a protective layer of HYD-3 to prevent the attack of chlorine ions. Finally, referring to the molecular structure of HYD-3, it can be inferred that the improvement in the surface morphology is due to the synergetic effect of aromatic rings and hydrazone group and, in particular, thanks to the presence of the two methoxy groups, which facilitate the adsorption of HYD-3 into the MS surface and therefore good inhibition action. These confirm results obtained from electrochemical analyses.

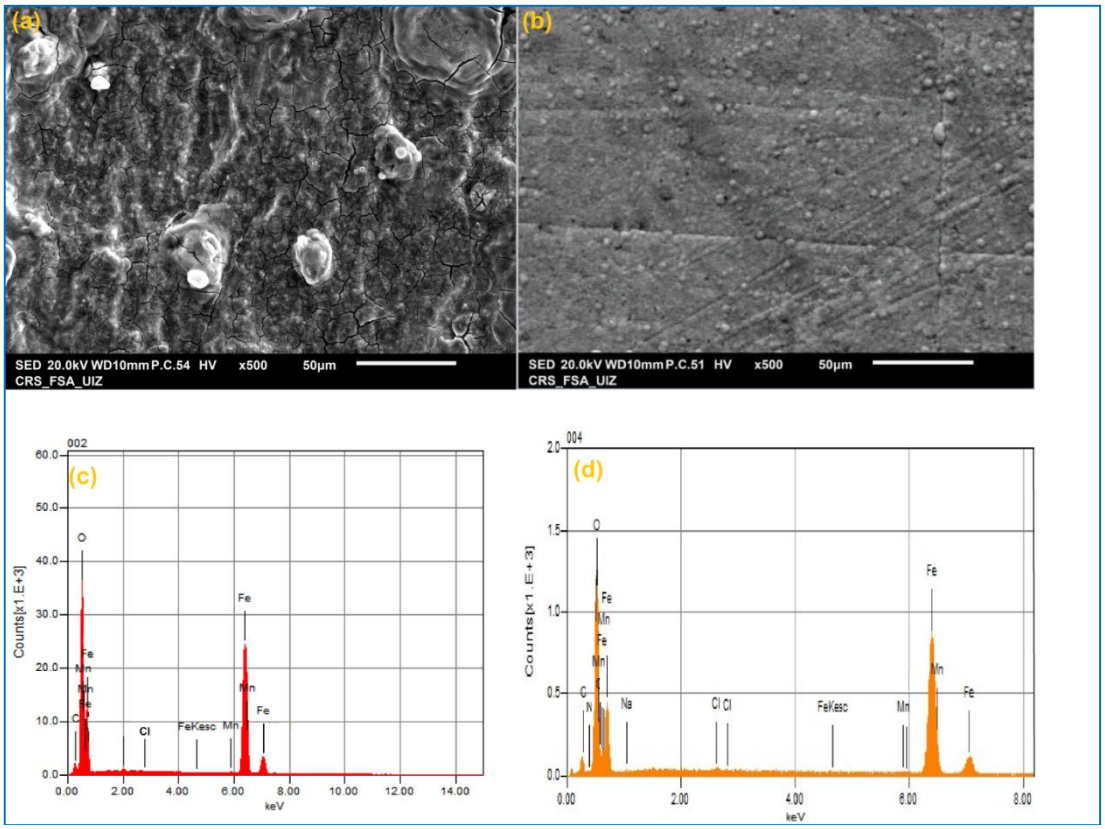

Figure 8. SEM and EDX images of MS samples after 24 hrs in blank (a, c) and inhibited solutions (5×10^{-3} M of HYD-3) (b, d).

3.6. Comparison with other hydrazone derivatives

Based on the literature, one can find several papers on corrosion inhibition of metals and alloys using hydrazone derivatives. This family of inhibitors has demonstrated their ability to inhibit metal corrosion. Thus, the design of compounds synthesized by hydrazone family attracts sustained scientific attention. The inhibition efficiency of some common representatives of the similar inhibitors is summarized in Table 10.

Table 10. Comparison of the inhibition efficiency of HYD-3 and HYD-4 compounds with the literature data based on other hydrazone derivatives as corrosion inhibitors for steel in acidic medium.

Inhibitor/ Concentration	Metal/ Medium	Inhibition efficiency (%)	Reference
2-ABNH / 6 mM	Mild steel/1 M HCl	95	[57]
E-NBPTH /10^{-3} M	XC48 C-steel /0.5M H_2SO_4	87	[58]
HZD^1/5x10^{-3} M	Mild steel/1 M HCl	97	[59]
HZD^2/5x10^{-3} M	Mild steel/1 M HCl	94	[59]
HZD^3/5x10^{-3} M	Mild steel/1 M HCl	92	[59]
HZD^4/5x10^{-3} M	Mild steel/1 M HCl	86	[59]
PTABH/400 mg L^{-1}	Mild steel/0.5M H_2SO_4	96	[60]
BZD-3 /5x10^{-3} M	MS/1 M HCl	93	Present work
BZD-4 /5x10^{-3} M	Mild steel/ 1 M HCl	91	Present work

4. CONCLUSION

In summary, two hydrazone derivatives, namely, (E)-N'-(4-methoxybenzylidene)-2-(6-methoxynaphthalen 2-yl)propanehydrazide (HYD-3) and N'-cyclohexylidene-2-(6-methoxynaphthalen-2-yl)propanehydrazide (HYD-4) have been synthesized and proposed as environment-friendly and effective inhibitors of mild steel in 1.0 M HCl solution. Overall, using different chemical and electrochemical methods, the following conclusions can be drawn:

- Studied HYDs acted as good corrosion inhibitors in acidic medium, and their inhibition activity is increased with the increase of inhibitors concentrations, with HYD-3 presents better inhibition efficiency.
- PDP and EIS results indicated that HYDs acted as mixed-type inhibitors and lead to increase polarization resistance even at a low concentration.
- HYDs derivatives can adsorb on the MS surface through physicochemical adsorption which follows the Langmuir isotherm model.
- SEM micrographs, coupled with EDX analysis, confirmed the adsorption of tested hydrazones into MS surface by inducing the formation of a protective layer that hinders anodic and cathodic reactions to protect MS during the corrosion process.

Together these results provide important insights into the important role of hydrazones derivatives to inhibit the mild steel corrosion. It can be noted that these important findings are more encouraging to pays attention to these types of inhibitors to understand the vital link between inhibition efficiency for studied molecules and their molecular structure properties. For this reason, to obtain further in-depth information about this relationship, theoretical studies based DFT and molecular dynamic simulations are going to be detailed in a forthcoming article to support and extend the understanding of the experimental results.

ACKNOWLEDGEMENTS
"The authors extend their appreciation to the Deanship of Scientific Research at King Khalid University for funding this work through research groups program under grant number R.G.P.1/199/41."

References

1. M. Yadav, L. Gope, N. Kumari, P. Yadav, *J. Mol. Liq.*, 216 (2016) 78–86.
2. H.B. Ouici, O. Benali, A. Guendouzi, *Res. Chem. Intermed.*, 42 (2016) 7085–7109.
3. F. Bentiss, M. Lagrenee, M. Traisnel, J. Hornez, *Corros. Sci.*, 41 (1999) 789–803.
4. S.K. Saha, M. Murmu, N.C. Murmu, P. Banerjee, *J. Mol. Liq.*, 224 (2016) 629–638.
5. N. Kovačević, A. Kokalj, *Corros. Sci.*, 53 (2011) 909–921.
6. A. Fouda, R. Fouad, *Cogent Chem.*, 2 (2016) 1221174.
7. D. Zhang, Y. Tang, S. Qi, D. Dong, H. Cang, G. Lu, *Corros. Sci.*, 102 (2016) 517–522.
8. C.B. Verma, M.A. Quraishi, A. Singh, *J. Taiwan Inst. Chem. Eng.*, 49 (2015) 229–239.
9. Y. Zhang, Y. Cheng, F. Ma, K. Cao, *Int. J. Electrochem. Sci.*, 14 (2019) 999–1008.
10. F. Bentiss, M. Outirite, M. Traisnel, H. Vezin, M. Lagrenée, B. Hammouti, S.S. Al-Deyab, C. Jama, *Int. J. Electrochem. Sci.*, 7 (2012) 1699–1723.
11. H. Lgaz, R. Salghi, I.H. Ali, *Int. J. Electrochem. Sci.*, 13 (2018) 250–264.
12. G. Koch, (2017).
13. X. Li, S. Deng, T. Lin, X. Xie, G. Du, *Corros. Sci.*, 118 (2017) 202–216.
14. D. Daoud, T. Douadi, H. Hamani, S. Chafaa, M. Al-Noaimi, *Corros. Sci.*, 94 (2015) 21–37.
15. I. Obot, D. Macdonald, Z. Gasem, *Corros. Sci.*, 99 (2015) 1–30.
16. A. Chaouiki, H. Lgaz, R. Salghi, M. Chafiq, H. Oudda, K. Bhat, I. Cretescu, I. Ali, R. Marzouki, I. Chung, *Colloids Surf. Physicochem. Eng. Asp.*, 588 (2020) 124366.
17. G. Bahlakeh, A. Dehghani, B. Ramezanzadeh, M. Ramezanzadeh, *J. Mol. Liq.*, 293 (2019) 111559.
18. S. Akbarzadeh, B. Ramezanzadeh, G. Bahlakeh, M. Ramezanzadeh, *J. Mol. Liq.*, 296 (2019) 111809.
19. Z. Sanaei, G. Bahlakeh, B. Ramezanzadeh, M. Ramezanzadeh, *J. Mol. Liq.*, 290 (2019) 111176.
20. A. Dehghani, G. Bahlakeh, B. Ramezanzadeh, M. Ramezanzadeh, *J. Mol. Liq.*, 279 (2019) 603–624.
21. A.K. Singh, E.E. Ebenso, M. Quraishi, *Int J Electrochem Sci*, 7 (2012) 2320.
22. A. Chaouiki, H. Lgaz, I.-M. Chung, I. Ali, S.L. Gaonkar, K. Bhat, R. Salghi, H. Oudda, M. Khan, *J. Mol. Liq.*, 266 (2018) 603–616.
23. G. Avci, *Mater. Chem. Phys.*, 112 (2008) 234–238.
24. G.N. Mu, X. Li, F. Li, *Mater. Chem. Phys.*, 86 (2004) 59–68.
25. N. Mamatha, N.S. Babu, K. Mukkanti, S. Pal, *Molbank*, 2011 (2011) M741.
26. A. Almasirad, M. Tajik, D. Bakhtiari, A. Shafiee, M. Abdollahi, M.J. Zamani, R. Khorasani, H. Esmaily, *J Pharm Pharm Sci*, 8 (2005) 419–425.

27. A. Chaouiki, M. Chafiq, H. Lgaz, M.R. Al-Hadeethi, I.H. Ali, S. Masroor, I.-M. Chung, *Coatings*, 10 (2020) 640.
28. J. Scully, R. Baboian, *ASTM Phila PA* (1995).
29. A. Standard, *Am. Soc. Test. Mater. G1-03* (2011).
30. A. Chaouiki, H. Lgaz, R. Salghi, M. Chafiq, H. Oudda, K. Bhat, I. Cretescu, I. Ali, R. Marzouki, I. Chung, *Colloids Surf. Physicochem. Eng. Asp.*, 588 (2020) 124366.
31. A. Chaouiki, H. Lgaz, S. Zehra, R. Salghi, I.-M. Chung, Y. El Aoufir, K.S. Bhat, I.H. Ali, S.L. Gaonkar, M.I. Khan, *J. Adhes. Sci. Technol.*, 33 (2019) 921–944.
32. H. Lgaz, S. Zehra, M. Albayati, K. Toumiat, Y. El Aoufir, A. Chaouiki, R. Salghi, I.H. Ali, M. Khan, I. Chung, *Int J Electrochem Sci*, 14 (2019) 6667–6681.
33. N. Anusuya, P. Sounthari, J. Saranya, K. Parameswari, S. Chitra, *J Mater Env. Sci*, 6 (2015) 1606–1623.
34. C.B. Verma, M. Quraishi, A. Singh, *J. Taiwan Inst. Chem. Eng.*, 49 (2015) 229–239.
35. P.M. Wadhwani, D.G. Ladha, V.K. Panchal, N.K. Shah, *RSC Adv.*, 5 (2015) 7098–7111.
36. A. Chaouiki, H. Lgaz, S. Zehra, R. Salghi, I.-M. Chung, Y. El Aoufir, K.S. Bhat, I.H. Ali, S.L. Gaonkar, M.I. Khan, *J. Adhes. Sci. Technol.*, 33 (2019) 921–944.
37. M. Messali, H. Lgaz, R. Dassanayake, R. Salghi, S. Jodeh, N. Abidi, O. Hamed, *J. Mol. Struct.*, 1145 (2017) 43–54.
38. D.B. Hmamou, R. Salghi, A. Zarrouk, H. Zarrok, R. Touzani, B. Hammouti, A. El Assyry, *J. Environ. Chem. Eng.*, 3 (2015) 2031–2041.
39. H. Lgaz, S.K. Saha, A. Chaouiki, K.S. Bhat, R. Salghi, P. Banerjee, I.H. Ali, M.I. Khan, I.-M. Chung, *Constr. Build. Mater.*, 233 (2020) 117320.
40. D.B. Hmamou, M. Aouad, R. Salghi, A. Zarrouk, M. Assouag, O. Benali, M. Messali, H. Zarrok, B. Hammouti, *J. Chem. Pharm. Res.*, 4 (2012) 3498–3504.
41. A.K. Singh, E.E. Ebenso, M. Quraishi, *Int J Electrochem Sci*, 7 (2012) 2320.
42. A.K. Singh, A.K. Pandey, P. Banerjee, S.K. Saha, B. Chugh, S. Thakur, B. Pani, P. Chaubey, G. Singh, *J. Environ. Chem. Eng.*, 7 (2019) 102971.
43. Y. El Aoufir, J. Sebhaoui, A. Chaouiki, H. Lgaz, R. Salghi, A. Guenbour, H. Oudda, E.M. Essassi, *J. Bio- Tribo-Corros.*, 4 (2018) 54.
44. A.O. Yüce, B.D. Mert, G. Kardaş, B. Yazıcı, *Corros. Sci.*, 83 (2014) 310–316.
45. E. Kowsari, S. Arman, M. Shahini, H. Zandi, A. Ehsani, R. Naderi, A. PourghasemiHanza, M. Mehdipour, *Corros. Sci.*, 112 (2016) 73–85.
46. L. Li, X. Zhang, J. Lei, J. He, S. Zhang, F. Pan, *Corros. Sci.*, 63 (2012) 82–90.
47. H. Lgaz, K.S. Bhat, R. Salghi, S. Jodeh, M. Algarra, B. Hammouti, I.H. Ali, A. Essamri, *J. Mol. Liq.*, 238 (2017) 71–83.
48. C. Verma, M. Quraishi, A. Singh, *J. Mol. Liq.*, 212 (2015) 804–812.
49. L.O. Olasunkanmi, M.F. Sebona, E.E. Ebenso, *J. Mol. Struct.*, 1149 (2017) 549–559.
50. M. Yadav, L. Gope, N. Kumari, P. Yadav, *J. Mol. Liq.*, 216 (2016) 78–86.
51. M.A. Quraishi, A. Singh, V.K. Singh, D.K. Yadav, A.K. Singh, *Mater. Chem. Phys.*, 122 (2010) 114–122.
52. F. Bentiss, M. Lagrenee, M. Traisnel, J. Hornez, *Corros. Sci.*, 41 (1999) 789–803.
53. H. Lgaz, I.-M. Chung, M.R. Albayati, A. Chaouiki, R. Salghi, S.K. Mohamed, *Arab. J. Chem.*, 13 (2020) 2934–2954.
54. S.R. Gupta, P. Mourya, M. Singh, V.P. Singh, *J. Organomet. Chem.*, 767 (2014) 136–143.
55. S. Umoren, U. Eduok, M. Solomon, A. Udoh, *Arab. J. Chem.*, 9 (2016) S209–S224.
56. N.V. Myung, D.-Y. Park, B.-Y. Yoo, P.T. Sumodjo, *J. Magn. Magn. Mater.*, 265 (2003) 189–198.
57. D.K. Singh, S. Kumar, G. Udayabhanu, R.P. John, *J. Mol. Liq.*, 216 (2016) 738–746.
58. N. Chafai, S. Chafaa, K. Benbouguerra, A. Hellal, M. Mehri, *J. Mol. Struct.*, 1181 (2019) 83–92.
59. H. Lgaz, A. Chaouiki, M.R. Albayati, R. Salghi, Y. El Aoufir, I.H. Ali, M.I. Khan, S.K. Mohamed, I.-M. Chung, *Res. Chem. Intermed.*, 45 (2019) 2269–2286.

60. A. Singh, S. Thakur, B. Pani, B. Chugh, H. Lgaz, I.-M. Chung, P. Chaubey, A. Pandey, J. Singh, *J. Mol. Liq.*, 283 (2019) 788–803.